ANALYSIS OF PORE DISTRIBUTION AND CONNECTIVITY IN CONCRETE USING X-RAY MICROTOMOGRAPHY

Zbigniew RANACHOWSKI[1*], Daria JÓŹWIAK-NIEDŹWIEDZKA[1], Przemysław RANACHOWSKI[1], Mariusz DĄBROWSKI[1], Stanislav KUDELA Jr.[2a], Tomas DVORAK[2]

[1] Institute of Fundamental Technological Research Polish Academy of Sciences 5B, Pawinskiego Str., 02-106 Warszawa, Poland, [2] Institute of Materials and Machine Mechanics, Racianska 75, 831- 02 Bratislava, Slovak Republic
e-mail: * zranach@ippt.pan.pl, a ummskudm@savba.sk

ABSTRACT

In the paper a method of X-ray microtomography (micro-CT) was employed for a direct insight into a microstructure of concrete with a practical resolution of approx. 10 micrometers^3. Two sets of specimens were subjects of examination. The spatial concentration of air pores was investigated in three concretes differing in the amount of the supplement of high calcium fly ash (HCFA). The parameter of pore connectivity called diffusive tortuosity was determined in three other concretes made of the same ingredients but differing in water to cement ratio. The quantitative results obtained with application of described procedures are applicable in material characterization.

Keywords
 X-ray microtomography, concrete, microstructure

INTRODUCTION

The research on durability of concrete outdoor objects is closely related to their properties of migration of potentialy harmful ionic fluids and aggresive gases what, in turn, relies on concrete mictostructure properties. The common methods of determining the latter are: the mercury intrusion porosimetry, nitrogen sorption and microscopic observations. X-ray microtomography (micro-CT) has the ability to create a 3D imaging of internal pore network with a resolution of ca. 1 - 5 um per voxel (volumetric pixel). The inventors of medical Computed Tomography were in 1979 Allan MacLeod Cormack and Godfrwey Newbold Hounsfield [1]. The early study of pore size distribution and of pore connectivity in concrete samples was performed by Lu *et al.* in 2005 and presented in [2].

Several papers concern the application of micro-CT technique in testing the properties of concrete. Garboczi [3] reconstructed the aggregate shapes with voxel resolution of 0.4 mm^3. This enabled the author to approximate the real shapes by its mathematical models to built the stereological model of entire population of aggregates. Lanzón *et al.* [4] used the micro-CT method to test the specimens made of concrete with low-density additions: expanded perlite, expanded glass and cenospheres (hollow microspheres). These additions varied significantly in parameters of their granulometric features. Capillary water absorption of prepared mortars was determined and compared with the reference mortar. The results of

physical measurements agreed with the volumetric pore concentration data obtained by processing of test results using micro-CT. Stock *et. al.* [5] analysed the progression of sulfate attack within the cement paste by examining the microtomograms. It was found that recognized damage levels in specimens exposed to a Na_2SO_4 solution in different conditions varied from 0 (no damage) to 4 (extreme damage).

Nakashima and Kamia [6] determined transport properties (i.e.: segmented porosity, surface to volume ratio of pores and difussion tortuosity of recognized pore system) in investigated porous rock piece. Provis et al. [7] tested the mixes of cement and siliceous fly ash and ground granulated blast furnace slag in different proportions after the ageing period of 4, 8, 16 and 48 days. The scanning was performed on agglomerates of particles of approx. 1 mm diameter with application of radiation from the high-energy synchrotrone source. Due to the use of a special source of radiation high resolution of 0.75 μm^3 at the tomograms was achieved. The aim of investigation was to trace the volume evolution of pores and to determine the time changes of connectivity within the pore system.

DETERMINATION OF PORE DISTRIBUTION IN CONCRETE SPECIMENS

The aim of presented research was to determine the volumetric and size distribution of pores in two concrete specimens of different porosity containing high calcium fly ash (HCFA) and in a reference specimen with no fly ash content. The refernce concrete mix was designed and prepared in a way to comply with the requirements of XC3 environmental exposition class (carbonation), The reference specimen contained no fly ash and the other mixes - 30% replacement of cement mass by HCFA.
Two kinds of HCFA were used:

- as delivered and unprocessed in specimen coded PW-NM-30,
- after sieve analysis with passing through 0.045 mm sieve in specimen coded PW-45-30.

HCFA was subjected to sieving in order to increase its grain specific surface and to remove unburned coal particles. The processed fly ash was characterized by specific density of 2.67 g/cm^3 , Blaine specific surface 3520 cm^2/g and fineness 20.8 %. The mixes were designed with the same water to binder ratio of 0.55. The same consistency was achieved by adding the proper amount of plasticizer. It was observed that the removal of the grain fractions above 45 μm improved the workability of the concrete mix, i.e. the less agglomerates containing the unburned coal particles remains in the prepared concrete mix the better workability of the prepared mixes. Sand of fraction 0 - 2 mm as fine aggregate and crushed amphibolite of fractions 2 - 8 and 8 - 16 mm as coarse aggregate were used. The cores of height of ca. 20 mm and of 20 mm diameter were drilled from the specimens described above to fulfil the requirements of the scanning procedure.

Micro-CT method was applied with Nanotom 30 microtomograph made by General Electric operating in the Institute of Materials and Machine Mechanics in Bratislava. The equipment was capable to produce the following three different data sets describing the specimen microstructure:

   1 - digital specimen images representing cross-sections of investigated object derived in transverse or lengthwise direction to the mean axis of the cylindrical sample,
   2 - lists of all pores detected in the specimen volume with specification of their coordinates, equivalent diameters and surfaces,

3 - three - dimensional projections of specimens with marked local pore concentrations presented by means of colour mappings.

The space resolution of the reconstructed microstructure was 10 μm^3 per voxel. The result of micro-CT scanning was a set of tomograms (specimen cross-sections), performed every 100 μm along the specimen height. The obtained digitized dataset included the information about the material brightness in arbitrary units [a.u.] for all voxels of core volume what was proportional to the local density of the material. The magnitudes of brightness were coded in following manner: the area of pores: 19 - 40 [a.u.], the mortar area: 41 - 100 [a.u.], aggregates: 101 - 255 [a.u.]. The other dataset was worked out with the use of the algorithm delivered by the producer of the equipment. It contained the position and dimensions of pores detected in the specimens and was capable to recognize pores within the effective diameter range of 30 - 1000 μm. The pores in that range contributed only to a part of total matrix porosity, capillary porosity was not taken into consideration. However the obtained information let the authors to find some differences in the microsrtucture of the investigated specimens.

The analysis of digital data characterizing the pores detected in specimen volume with specification of their coordinates allowed to determine the parameters related to the amount and distribution of pores in tested specimens. These parameters are smmarized in Table 1.

Table 1. Parameters of the porosity of the tested specimens

Material parameter	Specimen PW-0 (no addition of HCFA)	Specimen PW-NM-30 (addition of not sieved HCFA)	Specimen PW-45-30 (addition of sieved HCFA)
volumetric concentration of air pores	1.71 %	0.48 %	0.44 %
average distance between pores	194 μm	193 μm	121 μm
total number of pores	18183	6185	17901

Curves depicting the voxel brightness determined in mortars in three investigated specimens in relation to the current specimen height are presented in Fig. 1. The results allow to conclude that the mortar with no HCFA represents the highest brightness and thus the highest density. Therefore the replacement of the cement by HCFA results in the general loss of the density. On the contrary, the lowest density mortar origins from the specimen with not sieved HCFA. In Fig. 1 the local sharp brightness changes are caused by microcrakcs and other damages caused by cutting of the core, visible mostly at the both specimen edges.

On the basis of the data presented in Table 1 one can also conclude that the specimen with no HCFA replacement of cement was characterised by significantly higher volumetric concentration of air pores than the specimens with addition of HCFA. There is a considerable difference in number of pores in two latter concretes caused by the difference in implemented HCFA grain fineness. It is the evidence of the different pore diameter distribution in the specimens PW-NM-30 and PW-NM-45-30. The latter statement is illustrated by the volumetric pore diameter distribution of three investigated specimes, presented in Fig 2.
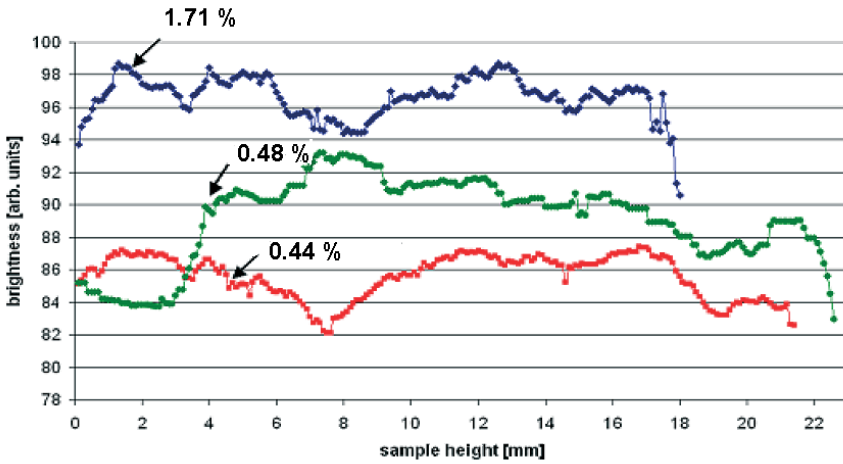
Fig. 1. The comparison of the averaged brightness of mortars of concretes described above, in relation to the current specimen height. The specimens are indentified by their volumetric concentration of air pores (in %) [8].
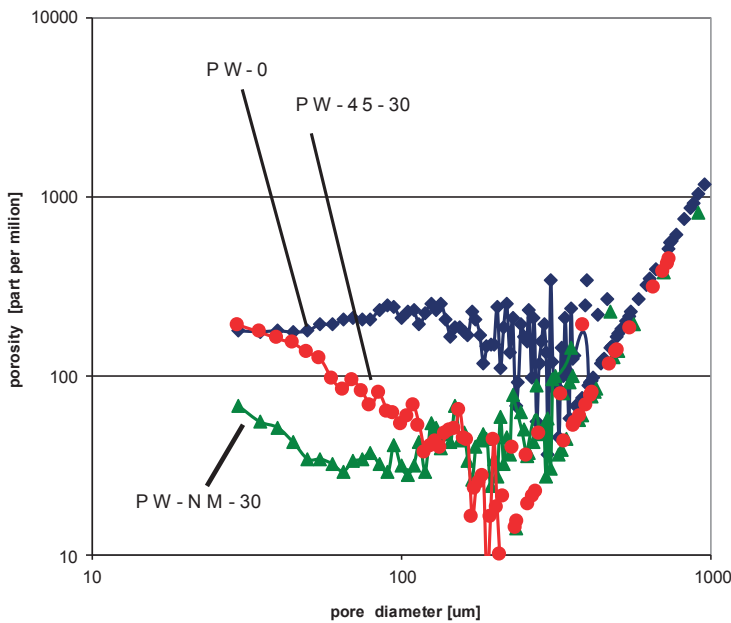
Fig. 2. Volumetric pore diameter distribution of three tested specimens. [8]

The results presented in Fig 2 allow to conclude that in the specimen with no HCFA addition there is more pores of diameter > 80 µm than in the other two specimens made with addition of HCFA. It is also clearly visible in Fig 2 that there are more pores of diameter < 100 µm in the specimen with finer HCFA grains, i.e. in PW-45-30 than in PW-NM-30

specimen. The concentration of pores > 300 μm   is for all the three specimens identical because of the limited diameter of HCFA grain.

THE ALGORITHM OF DETERMINING OF DIFUSSIVE TORTUOSITY

The scanning procedure of investigated specimen results in producing of binary datasets describing the consecutive specimen crosscections. In the case of prefering of 5 um^3 per voxel resolution and exact processing of a core of Φ 9 = mm and H = 9 mm cylinder the result is 1800 crossections of 2000 x 2000 of bytes each. The total number of bytes in such a dataset would be 7.2 G bytes what may cause the further processing durable. Therefore it is useful to take from the entire dataset a certain subset, preferably of cubic shape for further computations. The resulting subset is called a ROI (Region Of Interest) and is immune from the cracked areas situated in proximity of the specimen surface usualy damaged by a drilling tool. In described research it was decided to process 6 ROIs of 600^3 (216,000,000) voxels each. That way the ROIs represented cubes of 3 x 3 x 3 mm virtually extracted from investigated specimen. To analyse the   internal pore network connectivity a random walk algorithm [6] was implemented in a form of in-house prepared executable program for the PC computer.
       The latter algorithm was intended to simulate the diffusion of gases and liquids in the interconnected network of pores. At the starting point of the action a certain number of 'walkers' was distributed randomly across the processed ROI. The 'walkers' occupied one voxel of space and could be understood as a marked point in the dataset representing the analysed volume of the specimen. The walkers would migrate on neighbouring voxels obeying the information on voxels brightness (i.e. material density). The walkers would execute jumps in randomly chosen direction but the jumps could be performed if the neighbouring voxel belonged to a pore and otherwise the jumps were discarded.   After refreshing the position of all walkers, one epoch of its action has been completed by the algorithm. The number of epochs is measured by the dimensionless integer time *t*. The primary output of the random walk procedure was the walkers mean-square displacement $<r(t)^2>$ as a function of time (x_i, y_i, z_i are the coordinates of a current walker position and *n* is a number of operating walkers):

$$<r(t)^2>=\tfrac{1}{n} \sum_{i=1}^{n}[(x_i(t)-(x_i(0))^2+(y_i(t)-(y_i(0))^2 +(z_i(t)-(z_i(0))^2] \quad (1)$$

The the key transport property called diffusion tortuosity τ of the porous medium is related to the time-derivative of $<r(\tau)^2>$ and can be expressed as:

$$\tau = \frac{A}{d<r(t)^2>/dt} \ as \ t \rightarrow \infty \quad (2)$$

where *A* is a constant depended of implemented image lattice parameters and in [6, 7] is assumed as 1.
       The way of determining of τ as a converging limit of $d<r(\tau)^2>$ / *dt* needs the explanation. As time *t* elapsed random walkers migrated in porous media further than the average pore size. In the long - time limit they experienced the *tortuosity* of the surrounding material and the slope of $<r(\tau)^2>$ reached a constant value. Hence, the tortuosity is defined by (2). In practical condition to determine the slope $d<r(\tau)^2>/dt$ a specific procedure is using. It utilizes the calculation of the statistical coefficient of a least-squares linear regression using the consecutive 100 values of $<r(\tau)^2>$ taken for the large valuesof *t*. According to the

assumptions found in [7] in this paper it was applied 6000 walkers and the slope of $d<r(\tau)^2>/dt$ was checked in the proximity of $t = 400,000$ (i.e. for $t = 399100, 399101$ and so on...) for ten times. The resulting value of diffusive tortuosity was calculated as the average of the obtained results for wchich the correlation coefficient of the linear regression procedure is greater than 0.8.

The diffusive tortuosity is an idirect function of the porosity of the body. Below there will be discussed an example case to explain the properties of this parameter.The Figure 3. presents two model structures, both characterised by the volume fraction of porosity equalled 1 %. The porosity is represented by the rectangular channel crossing the central part of both structures. At the left side of the figure the channel possesses continuing interior and at the right side the channel is divided into two halves by thin obstacle. The tortuosity calculated with the program used in this research denoted 28 in the case of the long channel and denoted 56 for the obstacled variant.
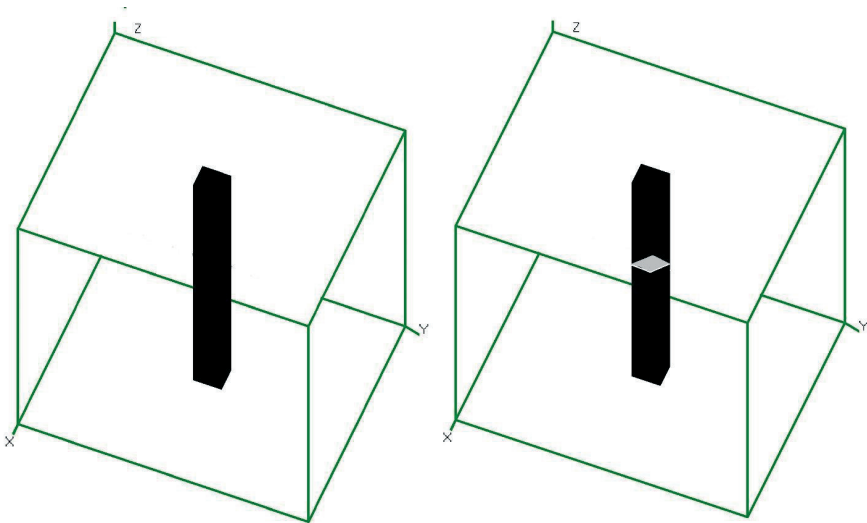

Fig. 3. Two model structures, of identical volume fraction of porosity (black pole in the center). The rectangular channel (left) has no discontinuities and the right side channel is divided into two halves by the thin obstacle [9].

EXAMINATION OF THE DIFFUSIVE TORTUOSITY
IN THREE CONCRETE SPECIMENS

For the need of present research, three concrete mixes were designed and prepared of the same ingredients but with different water to cement ratio to result in different level of porosity. Sand of fraction 0 - 2 mm as fine aggregate and crushed amphibolite of fractions 2 - 8 and 8 - 16 mm as coarse aggregate were used. The composition of concrete mixes is shown in Table 2.

Table 2. Composition of tested concretes, kg/m^3

Mix designa-tion	Cement CEM I 42.5 R	Fine aggregate 0-2 mm	Coarse aggregate 2-8 mm	Coarse aggregate 8-16 mm	Water	Superplas ticizer, % cement mass	Mix specific density [kg/m^3]
A	350	630	695	655	158	0.30	2424
B	400	580	625	615	200	0.00	2433
C	320	630	675	650	176	0.00	2431

The beams 100x100x500 mm were cast for and stored for 27 days in water at temperature of +22°C. Then they were stored at laboratory conditions at +20°C, 60% RH until the mass equilibrium was reached (14 days). The space resolution of the reconstructed microstructure during micro-CT scanning was 5μm^3 per voxel. Fig. 4 depicts the reconstructed 3D view of the processed cores of 9 mm in diameter, cut off the specimens.
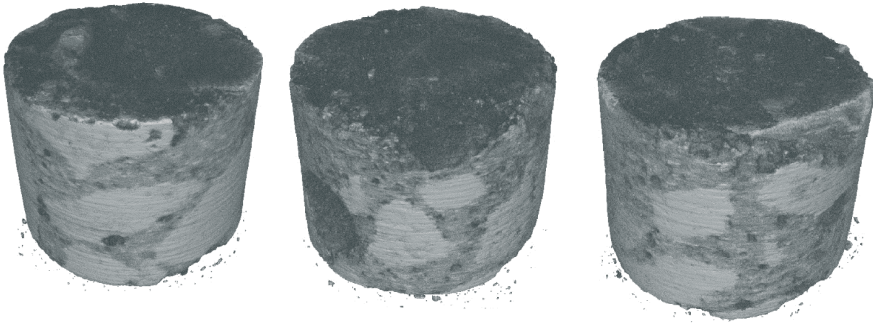

Fig. 4. Reconstructed from micro-CT, 3D view of the cores of 9 mm in diameter cut off tested specimens specified in Table 2.

The result of micro-CT scanning was a set of specimen cross-sections, performed every 5 µm along the specimen height. Two data subsets (ROIs) of 600^3 voxels were extracted from the datasets representing the specimens. Average cement matrix to aggregate ratio of ca. 40 % was determined in these subsets. The ROIs labelled A1, B1 and C1 are presented of Fig. 5. To determine the impact of cement matrix content in investigated ROIs to the results of calculating of tortuosity, the other group, labelled A2, B2 and C2 was prepared in such a way to obtain cement matrix to aggregate ratio of ca. 30 % what is depicted in Fig. 6.

In order to determine magnitudes of brightness of voxels belonging to pores, cement matrix and aggregates, greyscale value histograms were performed for all ROIs. These histograms are presented in Fig. 7. After the determination of greyscale levels related to three principal material phases it was possible to process the prepared ROIs using the algorithm of random walk presented in previous paragraph. The graphical illustration of the traces of walkers migration within the ROIs of type 1 is presented in Fig. 8. The visualisation was made after 400,000 of time steps. The final positions of first 500 walkers are marked with small dots.
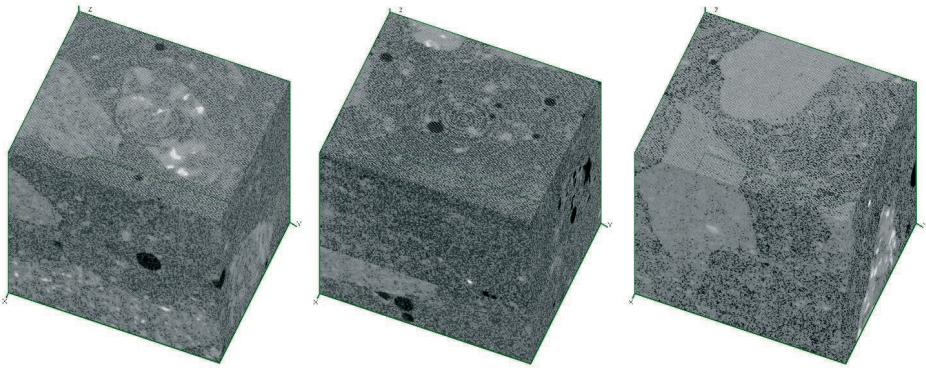
Fig. 5. The ROIs labelled A1, B1 and C1- representing specimen areas with cement matrix to aggregate ratio of ca. 40 % [9].
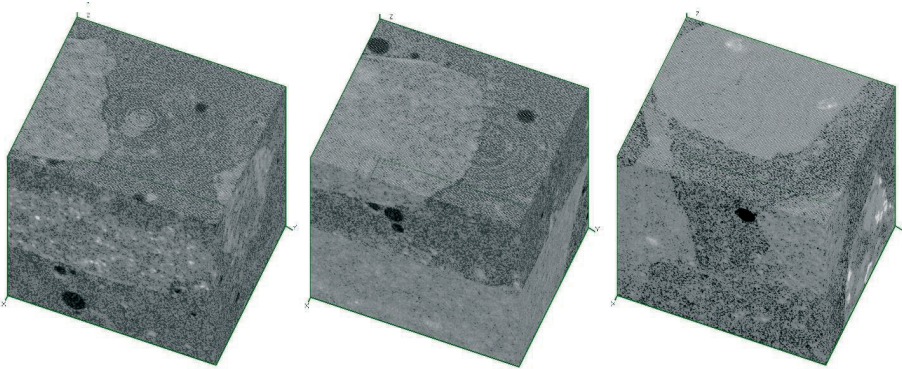

Fig. 6. The ROIs labelled A2, B2 and C2 representing specimen areas with cement matrix to aggregate ratio of ca. 30 % [9].

In histograms presented in Fig. 7 one can notice distinct discontinuities at the curves resulted by the transition from one material phase to another (i.e. pores-matrix-aggregates) what was discussed in [8]. It is obvious that the magnitude of the discontinuities depends on the volume distribution of phases in investigated piece of the material. On the basis of the greyscale histograms presented above the it was decided to take the following average brightness levels to distinguish the phases within analysed ROIs: 40 as the pores-matrix transition and 70 as the matrix-aggregates transition. It was proven that the variations made on these levels in magnitude of 2 or 4 percent have little influence for further determination of microstructural parameters.

For each ROI the ratio of pore volume to matrix volume was determined. The latter parameter called 'segmented porosity' can be used to characterize the concrete microstructure. The results of the analysis of the data obtained from the specimens by means of micro-CT method are summarized in Table 3.
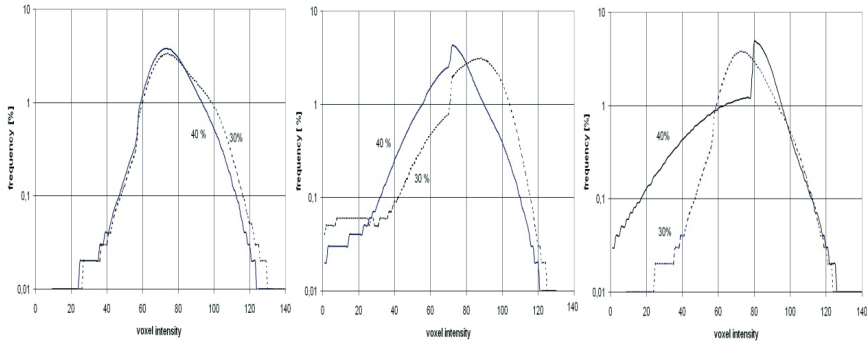
Fig. 7. Greyscale value histograms for all examined ROIs (left: specimen A, center: specimen B and right: specimen C, the labels denote the cement matrix to aggregate ratio of the ROI) [9]. The horizontal scale: voxel intensity [arb. units], the vertical scale: occurrence frequency [%].
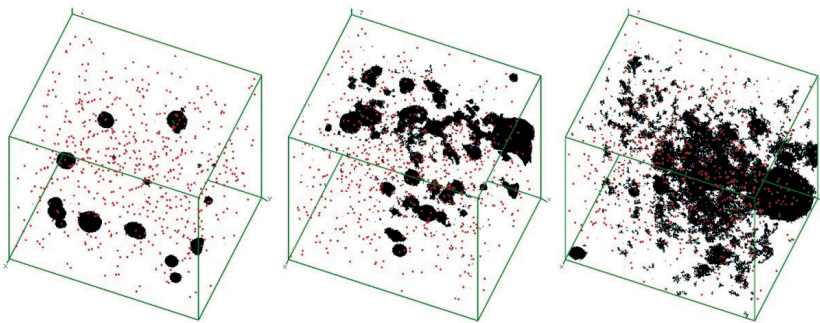

Fig. 8. Traces of paths taken by the walkers through the tortuous pore network of ROIs of type A1, B1 and C1 [9].

Table 3. Parameters related to the porosity of the tested specimens, determined on the basis of micro-CT method

Material parameter	Specimen A	Specimen B	Specimen C
water to cement ratio	0.45	0.5	0.55
pore to matrix volume in specimen part with cement matrix to aggregate ratio of ca. 40 %	0.8 %	4 %	18 %
pore to matrix volume in specimen part with cement matrix to aggregate ratio of ca. 30 %	0.8 %	2 %	17 %
diffusive tortuosity in specimen part with cement matrix to aggregate ratio of ca. 40 %	282	43	81
diffusive tortuosity in specimen part with cement matrix to aggregate ratio of ca. 30 %	244	96	46

CONCLUSIONS

The micro-CT method is capable to deliver information on the microstructure of tested concrete specimens after contactless and relatively fast inspection. The important point of the data analysis is the proper determination of the pores-matrix threshold and matrix-aggregates threshold in respect to the population of examined voxel brightness parameter. After the assumption of the latter parameter it is possible to determine the segmented (i.e observed) porosity what is proportional to the material porosity. It is also possible to calculate the diffusive tortuosity - the parameter describing the pore connectivity of the investigated material. However that latter parameter presents non-linear dependence on segmented porosity as it was discussed in [8] because it is sensitive to the configuration of pore system. In this paper the relation of segmented porosity to w/c parameter was found for specimens of w/c equalled 0.5 and 0.45 but this parameter was of significant different magnitude for specimen with higher w/c ratio. The procedure of determining of diffusive porosity resulted in a relatively large deviation of results and perhaps need more repetitions. However it is evident that combined with segmented porosity the diffusive tortuosity can be useful for determining of microstructural parameters of concrete.

ACKNOWLEDGMENTS

REFERENCES

1. Ratajczyk, E., Industrial Computer Tomography - types, performance, application, resolution [in Polish]. Measurement, Automation and Monitoring, Journ. of Metrological Section of Polish Technical Society SIMP, ISSN 0032-4140, 9, 2014, 713-717
2. Lu, S., Landis, E., Keane D., X-ray microtomographic studies of pore structure and permeability in Portland cement concrete. Materials and structures, 39, DOI: 10.1617/s11527-006-9099-1, 2006, 611-620
3. Garboczi, E.J., Three-dimensional mathematical analysis of particle shape using X-ray tomography and spherical harmonics: Application to aggregates used in concrete. Cement & Concrete Research, 32, 2002, 1621-1638
4. Lanzon, M., Cnudd,e V., de Kock, T., Dewanckele, J., X-ray microtomography (μ-CT) to evaluate microstructure of mortars containing low density additions. Cement & Concrete Composites, 34, 2012, 993-1000
5. Stock, S.R., Naik, N.K., Wilkinson, A.P., Kurtis, K.E., X-ray microtomography (micro-CT) of the progression of sulfate attack of cement paste. Cement & Concrete Research, 32, 2001, 1673-1675
6. Nakashima, Y., Kamia, S., Mathematica Programs for the Analysis of Three-Dimensional Pore Connectivity and Anisotropic Tortuosity of Porous Rocks using X-ray Computed Tomography Image data. J. of Nuclear Science and Technology, 44,9, 2012, 1233-1247
7. Provis, J.L., Myers, R.J., White, C.E., X-ray microtomography shows pore structure and tortuosity in alkali-activated binders. Cem. & Concr. Res., 2012, pp 42, 855 – 864
8. Ranachowski, Z., et al., Application of X-ray microtomography and optical microscopy to determine the microstructure of concrete penetrated by carbon dioxide. Arch. of Metall. and Mat., 59, 4, 2014, 1451-1457
9. Ranachowski, Z., Jóźwiak-Niedźwiedzka, D., Ranachowski, P., Dąbrowski, M., Kudela, S. Jr., Dvorak, T., The Determination of Diffusive Tortuosity in Concrete Specimens Using X-Ray Microtomography. Arch. of Metall. and Mat., 60, 2, 2015, 1115-1119